American Mineralogist, Volume 72, pages 329–336, 1987

Theoretical analysis of cation ordering in binary rhombohedral carbonate systems

Benjamin P. Burton

Alloy Phase Diagrams Data Center, Division 450, Room B150, Building 223,
National Bureau of Standards, Gaithersburg, Maryland 20899, U.S.A.

Abstract

A three-parameter version of the tetrahedron approximation in the cluster-variation method is used to model cation ordering in rhombohedral carbonate systems. The model is sufficient to calculate theoretical phase diagrams that are in complete qualitative agreement with high-temperature phase-equilibrium data and with experimental composition and temperature dependence of the excess heats that are associated with cation ordering. In addition, the many-body interaction parameters that are required to obtain appropriate phase-diagram topologies at high temperature lead to the prediction of an ordered ground-state with stoichiometry $Ca_3Mg(CO_3)_4$. Cation ordering in this 3:1 phase yields a trigonally distorted analogue of the Cu_3Au or Al_3Ti structure.

Introduction

Burton and Kikuchi (1984) presented a model that describes equilibrium subsolidus phase relations between calcite- and dolomite-structure phases in binary carbonate systems. This model is based on the tetrahedron approximation (TA) of the cluster-variation method (CVM) and will be referred to as the TA or CVM-TA. The present paper updates and improves upon this earlier work, particularly with respect to a high-temperature stability field in which two calcite-structure phases coexist. Such a field is observed experimentally in the systems $(1 - X)CaCO_3$-$XMgCO_3$, $(1 - X)CdCO_3$-$XMgCO_3$, $(1 - X)CaCO_3$-$XMnCO_3$, and $(1 - X)CaCO_3$-$XZnCO_3$ (Goldsmith, 1983, and references therein), but was absent from the calculated diagrams presented in Burton and Kikuchi (1984). In the previous paper we argued that an additional configurational degree of freedom is required to generate such a field, but the results presented below indicate that this argument is wrong and that a three-parameter version of the TA is sufficient to calculate phase diagrams that are in complete qualitative agreement with experiment. The model also predicts systematics (composition and temperature dependence) for the excess heat of solution $\Delta H^{xs}(X,T)$ that are in qualitative agreement with recent thermochemical measurements (Capobianco and Navrotsky, 1985; Capobianco, 1986; Capobianco et al., 1987).

Burton and Kikuchi (1984) showed that most features of the experimental phase diagrams are present in calculated diagrams if one assumes that the interactions that cause cation ordering are highly *anisotropic* such that ordering is favored parallel to the hexagonal **c** axis ($\mathbf{c}_h$, i.e., between hexagonal basal layers) but clustering is favored parallel to $\mathbf{a}_h$ (within basal layers). The results presented below fully support this assumption, but they also put increased emphasis on the *many-body interactions* that cause the phase diagram to be asymmetric about $X = 0.5$ and make it possible for a field with two calcite-structure phases to occur. In particular, the many-body interaction parameters that produce appropriate phase-diagram topologies at high temperature imply negative excess heats of mixing in the compositional range $X \lesssim 0.3$, and this leads to the prediction that additional ordered phases may occur in Ca- or Cd-rich solutions. The most prominent additional phase is based on 3:1 stoichiometry [e.g., $Ca_3Mg(CO_3)_4$] and has a structure that can be regarded as a trigonally distorted analogue of the Cu_3Au structure.

Background

Crystal structures

In calcite, the Ca^{2+} ions occupy a trigonally distorted fcc array of sites (shortened along one of the three $\langle 111 \rangle_{fcc}$ vectors), and CO_3^{2-} groups occupy the octahedral interstices. Threefold axes of the CO_3^{2-} groups are parallel to the shortened $\langle 111 \rangle_{fcc}$ vector, and groups in alternate $(111)_{fcc}$ layers are rotated by 180° relative to one another. In dolomite, Ca^{2+} and Mg^{2+} preferentially occupy alternate $(111)_{fcc}$ planes, which become crystallographically distinct α- and β-hexagonal basal planes, or Ca and Mg layers. Thus, the dolomite structure may be regarded as a trigonally distorted analogue of the CuPt structure. Some additional ordered phases [3:1, 2:1, 5:1, and "γ-" and "δ-dolomite" (Wenk and Zhang, 1985)] are also considered, and their structures are described below. All of these structures, except δ-dolomite, are derived from calcite by ordering of cations both *between* and *within* hexagonal basal layers.

The 3:1 phase is characterized by ordering within basal planes such that rows of Ca-Mg-Ca- . . . sites alternate with rows of Ca-Ca-Ca . . . sites, parallel to $\mathbf{a}_h$. All basal

0003–004X/87/0304–0329$02.00

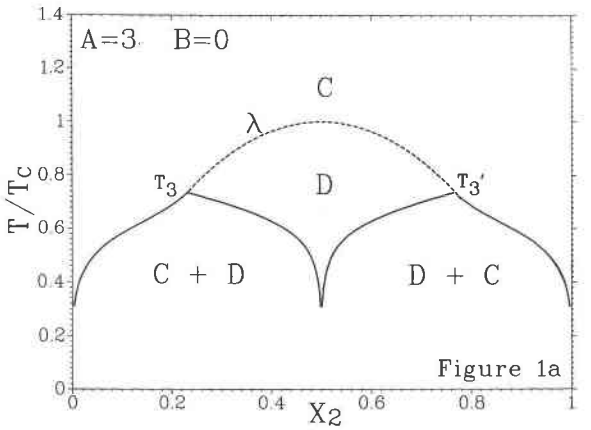

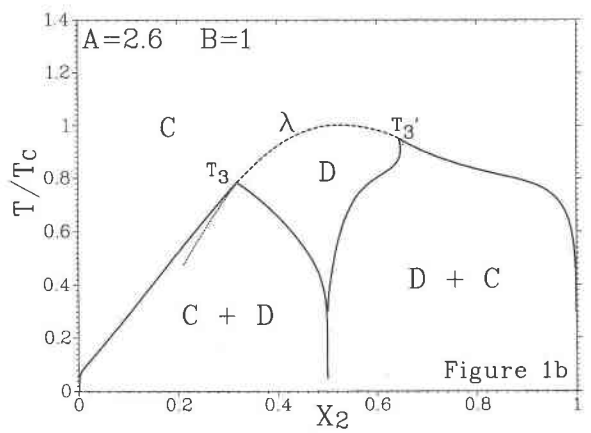

Fig. 1. (a) The symmetrical composition vs. temperature diagram ($\epsilon_{ier} = -1$, $\epsilon_{ira} = 3$); C = calcite-structure phase, D = dolomite-structure phase. (b) asymmetrical diagram, calculated with ϵ_{ijkl}, $A = 2.6$, and $B = 1$.

layers have the same intralayer ordering, and adjacent layers are arranged in such a way that no Mg site has an Mg site as a nearest neighbor (nn) in an adjoining layer. This ordering scheme maximizes the number of Mg–Ca nn's both between and within basal layers, and it preserves the space-group symmetry of calcite ($R\bar{3}c$), but with $\mathbf{a}_h(3{:}1) = 2\mathbf{a}_h$(calcite). Thus, the 3:1 phase has a structure that may be regarded as a trigonally distorted analogue of the Cu_3Au structure. Another possible ordering scheme, with 3:1 stoichiometry, has Ca layers alternating with (CaMg) layers in which rows of Ca sites ($\| \mathbf{a}_h$) alternate with rows of Mg sites, and there is some experimental evidence for this type of intralayer ordering ("c" reflections discussed by Van Tendeloo et al., 1985; referred to as "γ-dolomite" by Wenk and Zhang, 1985). The γ-dolomite ordering maximizes the number of interlayer Mg–Ca nn's, but not the number of intralayer Mg–Ca nn's. (See note added in proof.)

In the 2:1 phase, all basal layers are ordered in such a way that a honeycomb array of Ca sites surrounds the Mg sites within basal layers, and the orientation of adjacent layers minimizes the number of Mg sites with nn Mg sites on adjoining layers. The δ-dolomite phase reported by Wenk and Zhang (1985) also has 2:1 stoichiometry, but its structure does not involve intralayer ordering; δ-dolomite is derived from dolomite by doubling each of the Ca layers, so that the layer sequence along $\mathbf{c}_h$ is Mg-Ca-Ca-Mg- . . . .

The 5:1 phase has honeycomb layers, as in the 2:1 phase, that alternate with Ca layers.

Experimental phase-diagram topologies

Experimental phase diagrams for the systems $(1 - X)CaCO_3$-$XMgCO_3$ and $(1 - X)CdCO_3$-$XMgCO_3$ [and probably $(1 - X)CaCO_3$-$XMnCO_3$ as well; Goldsmith, 1983] exhibit the following characteristics: (1) D field—a narrow stability field, based on $X = 0.5$ stoichiometry in which a dolomite-structure phase is stable (space group $R\bar{3}$); (2) C field—a high-temperature region of continuous solubility above the D field, implying an ordering transition that relates the D phase to a higher-temperature C phase (space group $R\bar{3}c$); (3) C + D and D + C fields—broad two-phase fields flanking the D field in which the D phase coexists with a C phase of different composition; (4) $C_1 + C_2$ field—a broad two-phase field, at temperatures higher than the D + C field, in which two C phases coexist.

The CVM-TA calculations reported in Burton and Kikuchi (1984) and those described below, typically produce the combination of characteristics (1)–(3) and (1)–(4), respectively, in combination with a second-order phase transition relating the C and D phases. Phase-diagram topologies involving a first-order transition typically arise in combination with a broad D field flanked by narrow C + D and D + C fields and in the absence of a $C_1 + C_2$ field. Therefore, calculated phase diagrams (Figs. 1–4) exhibit lines of second-order transition (λ lines) and multicritical points (tricritical points and critical end points)[1] at the intersections between λ lines and two-phase fields.

The model

A derivation of the CVM-TA was presented in Burton and Kikuchi (1984) and is not repeated here. The only significant difference between the calculations discussed below and those reported in Burton and Kikuchi (1984) is in the expression for the configurational contribution to the internal energy, which is expressed as a product of concentration variables and internal energies per tetrahedron,

$$\Delta E = 2 \sum_{ijkl} [X(4, \alpha)_{ijkl} + X(4, \beta)_{ijkl}]\epsilon_{ijkl}. \qquad (1)$$

Indices i, j, k, and l are equal to 1 or 2 and indicate species 1 or 2, respectively ($1 = Ca^{2+}$, $2 = Mg^{2+}$); $X(4,\alpha)_{ijkl}$ and $X(4,\beta)_{ijkl}$ are the concentrations of tetrahedral clusters with site configurations $\{\alpha\alpha\alpha\beta\}$ and $\{\beta\beta\beta\alpha\}$, respectively[2]

[1] For a detailed discussion of the distinction between a tricritical point and a critical end point, see Allen and Cahn (1982).

[2] For example, $X(4,\alpha)_{1112}$ is the concentration of α tetrahedra with three Ca^{2+} on α sites and one Mg^{2+} on a β site (note that indices i, j, and k always refer to sites in the same basal plane).

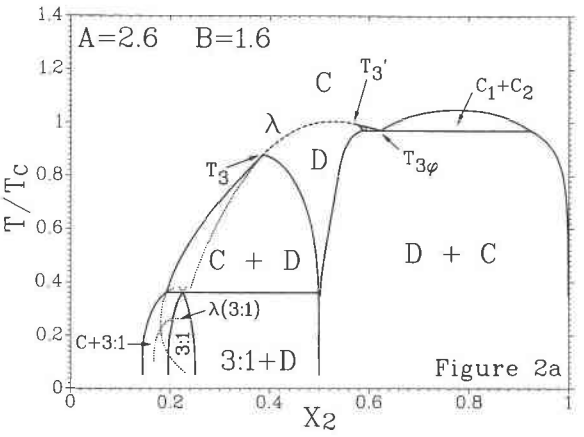

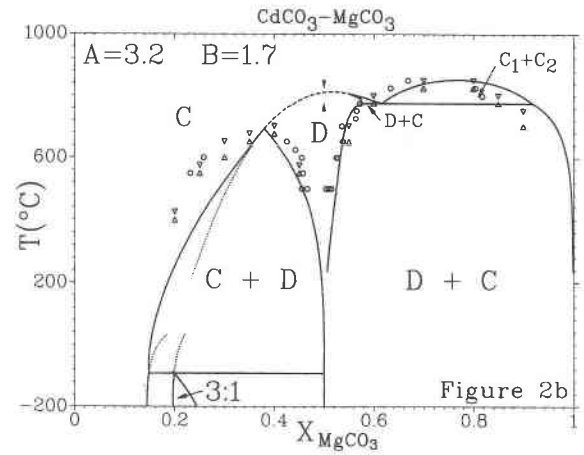

Fig. 2. (a) Calculated composition vs. temperature diagram ($\epsilon_{ier} = 1$, $A = 2.6$, $B = 1.6$), illustrating the "cone" topology. (b) A comparison of calculated ($\epsilon_{ier} = -1$, $A = 3.2$, $B = 1.7$) and experimental (data points from Goldsmith, 1972) diagrams for the system $CdCO_3$-$MgCO_3$.

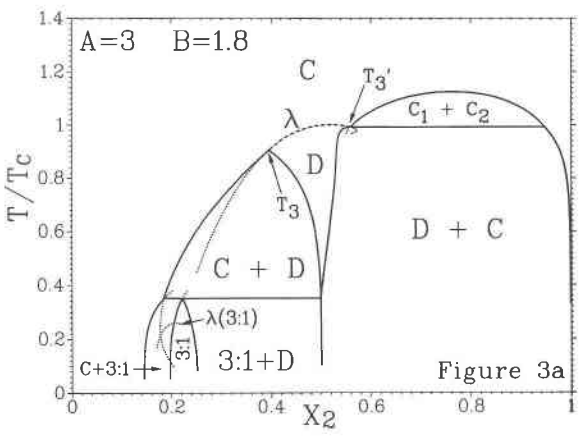

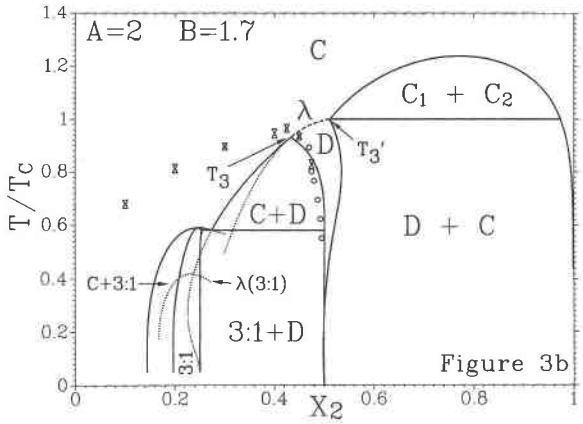

Fig. 3. (a) Calculated compositions vs. temperature diagram ($\epsilon_{ier} = -1$, $A = 3$, $B = 1.8$) illustrating the critical-end-point (T_3') topology. (b) Composition vs. temperature diagram ($\epsilon_{ier} = -1$, $A = 2$, $B = 1.7$). Data points are from Goldsmith and Heard (1961).

(in dolomite, α sites are preferentially occupied by Ca^{2+} and β sites by Mg^{2+}); ϵ_{ijkl} is the configurational internal energy of a tetrahedral cluster in configuration $\{ijkl\}$; and the factor of two preceding the summation sign is present because ΔE is normalized for a system of $2N_0$ sites (N_0 is Avogadro's number, and in a system of $2N_0$ cations there are $2N_0$ α tetrahedra plus $2N_0$ β tetrahedra).

Burton and Kikuchi (1984) showed that one can generate symmetrical phase diagrams, of the type shown in Figure 1a, by parameterizing ϵ_{ijkl} as a function of two pairwise interaction parameters, ϵ_{ier} and ϵ_{ira}, such that

$$\epsilon_{ijkl} = (1/2)(n_{ijkl}\epsilon_{ier} + m_{ijkl}\epsilon_{ira}) \qquad (2)$$

where $n_{ijkl} \equiv |i-l| + |j-l| + |k-l|$ = the number of *inter*layer 1–2 nn's and $m_{ijkl} \equiv |i-j| + |j-k| + |k-i|$ = the number of *intra*layer 1–2 nn's. The factor of (1/2) is present in Equation 2 because each pair is shared by two tetrahedra; ϵ_{ier} is the energy of formation of a 1–2 nn pair in which the Ca^{2+} and Mg^{2+} ions occupy sites on adjacent basal layers [$(1)^\alpha$–$(2)^\beta$ or $(2)^\alpha$–$(1)^\beta$ "*inter*layer pairs"]; ϵ_{ira} is the energy of formation for nn pairs in which both cations occupy sites in the same basal layer [$(1)^\alpha$–$(2)^\alpha$ or $(1)^\beta$–$(2)^\beta$ "*intra*layer pairs") in configuration $\{ijkl\}$.

Note that $\epsilon_{ier} < 0$ implies that the total energy is decreased by the formation of $(1)^\alpha$–$(2)^\beta$ or $(2)^\alpha$–$(1)^\beta$ interlayer pairs and $\epsilon_{ira} > 0$ implies that the total energy is increased by the formation of $(1)^\alpha$–$(2)^\alpha$ or $(1)^\beta$–$(2)^\beta$ intralayer pairs, hence, the simultaneous occurrence of both ordering and phase separation. Also note that in perfectly ordered stoichiometric dolomite, all interlayer pairs are in configuration $(Ca^{2+})^\alpha$–$(Mg^{2+})^\beta$, and all intralayer pairs are in configurations $(Ca^{2+})^\alpha$–$(Ca^{2+})^\alpha$ and $(Mg^{2+})^\beta$–$(Mg^{2+})^\beta$.

To break the symmetry of the phase diagram shown in Figure 1a, Burton and Kikuchi (1984) used many-body interaction parameters, δ_{ier} and δ_{ira}, which have the effect of making ϵ_{ier} and ϵ_{ira} functions of the concentration of Mg^{2+} in configuration $\{ijkl\}$, i.e., functions of $i + j + k + l$. Specifically, Equation 16 in Burton and Kikuchi expressed ϵ_{ijkl} as

$$\epsilon_{ijkl} = (1/2)\{n_{ijkl}[\epsilon_{ier} + (\eta_2 - 2)\delta_{ier}] + m_{ijkl}[\epsilon_{ira} + (\eta_2 - 2)\delta_{ira}]\}, \qquad (3a)$$

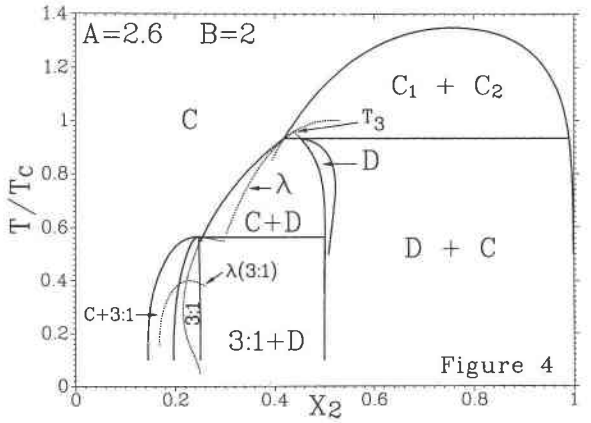

Fig. 4. Calculated composition vs. temperature diagram ($\epsilon_{ier} = -1$, $A = 2.6$, $B = 2$) illustrating the λ-metastable topology.

where $\eta_2 \equiv i + j + k + l - 4$ = the number of Mg^{2+} in configuration $\{ijkl\}$. (3b) Calculations based on this formulation did produce asymmetric phase diagrams, but in all cases investigated the λ line pierced the peaks of both the C + D and D + C fields, and the $C_1 + C_2$ field was absent. The model is, however, capable of generating appropriate phase-diagram topologies. For example, the diagrams shown in Figures 1–4 were calculated with

$$\epsilon_{ier} = -1 \text{ (in dimensionless units)} \quad (4a)$$

$$\epsilon_{ira} = A + (\eta_2 - \eta_1)B \quad (4b)$$

$$\eta_1 \equiv 8 - i - j - k - l = 4 - \eta_2. \quad (4c)$$

In Equations 4a–4c, η_1 = the number of Ca^{2+} in configuration $\{ijkl\}$, A is the intralayer repulsion parameter, a positive constant, and B is a many-body interaction parameter, also a positive constant. An increase in B implies an increased departure from the symmetric phase diagrams that occur when $B = 0$ (Fig. 5a).

Results and discussion

Ground states

In the CVM-TA, ground-state energies for ordered phases are calculated by counting the number (concentration) of tetrahedra in a given $\{ijkl\}$ configuration and multiplying by ϵ_{ijkl}. For example, the ground-state energy, *per tetrahedron,* for stoichiometric dolomite is

$$\Delta E_D = (\epsilon_{1112} + \epsilon_{2221})/2 = -3/2. \quad (5a)$$

Similarly, the ground-state energies, per tetrahedron, for the stoichiometric 3:1, γ-dolomite, 2:1, δ-dolomite, and 5:1 phases are

$$\Delta E_{3:1} = (3\epsilon_{2111} + \epsilon_{1112})/4 = 3(A - 2B - 1)/4 \quad (5b)$$

$$\Delta E_\gamma = (\epsilon_{2111} + \epsilon_{2211} + \epsilon_{1111} + \epsilon_{1112})/4 = (2A - 2B - 3)/4 \quad (5c)$$

$$\Delta E_{2:1} = (2\epsilon_{2111} + \epsilon_{2112})/3 = (3A - 4B - 2)/3 \quad (5d)$$

$$\Delta E_\delta = (\epsilon_{1112} + \epsilon_{2221} + 2\epsilon_{1111})/4 = -3/4 \quad (5e)$$

$$\Delta E_{5:1} = (9\epsilon_{2111} + \epsilon_{1112} + 2\epsilon_{1111})/12 = (A - 2B - 1)/2. \quad (5f)$$

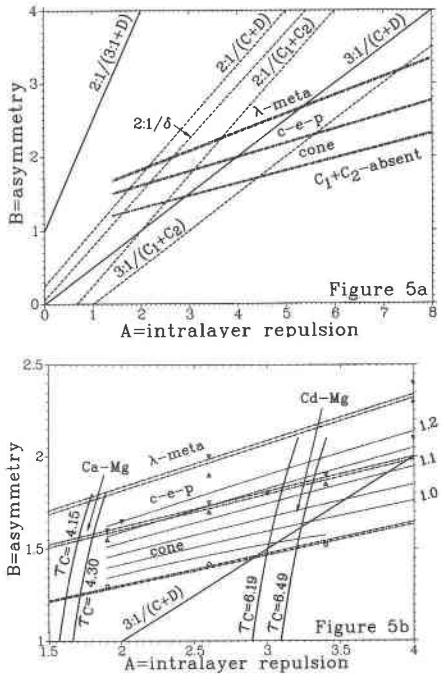

Fig. 5. (a) The parameter space for models based on the CVM-TA and Equations 4a–4c ($\epsilon_{ier} = -1$, $A \geq 0$, and $B \geq 0$). The double dash-dot lines indicate approximate boundaries between fields for the four different phase-diagram topologies (Figs. 1–4). Solid lines define regions in which the 2:1 and 3:1 phases are stable ground states. Dashed lines define regions in which various metastable equilibria may occur. (b) A portion of the same parameter space with certain quantitative constraints included. Dotted lines labeled 1.2, 1.1, and 1.0, are contours of constant ratio T_{cons}/T_C = (consolute temperature of the $C_1 + C_2$ field)/(T_C for dolomite). Solid, nearly vertical curves indicate values of τ_C (Table 2) that are consistent with thermochemical data and experimental T_C values. Arrows indicate approximate locations of best fit for the Ca-Mg and Cd-Mg systems. Triangles indicate calculations that bracket the regions for different phase-diagram topologies. Circles indicate linearly extrapolated values of B at which $T_{cons}/T_3' \rightarrow 0$, when ϵ_{ier} and A are held constant.

Equations 5a–5f were used to calculate the solid and dashed lines in Figure 5a that define 0-K stability fields (in parameter space) for the different ordered phases. For example, the line labeled 3:1/(C + D) (Fig. 5a) can be determined as follows: first evaluate the energy of a C + D mechanical mixture, at the composition of the stoichiometric 3:1 phase,

$$\Delta E_{C+D}(X = \tfrac{1}{4}) = (\Delta E_C + \Delta E_D)/2 = (2\epsilon_{1111} + \epsilon_{1112} + \epsilon_{2221})/4 = -\tfrac{3}{4} \quad (6a)$$

(note $\Delta E_C = \epsilon_{1111} = \epsilon_{2222} = 0$); then solve the inequality,

$$\Delta E_{3:1} \leq -\tfrac{3}{4}, \quad (6b)$$

which is the condition for stability of the 3:1 phase relative to C + D. Substituting Equation 5b into 6b, and solving for B yields

$$B \geq A/2. \quad (6c)$$

TABLE 1. Approximate locations of special points in experimental phase diagrams

System	X_3	X_3'	T_3/T_C	T_3'/T_C	T_{cons}/T_C	T_C (°C)	Ref.
$CaCO_3$-$MgCO_3$	0.41–0.44	0.52–0.55	0.96	?	1.1–1.3	1100–1150	1
$CdCO_3$-$MgCO_3$	0.38–0.41	0.57–0.60	0.89	0.98	1.02	775*–≤825	2
$CaCO_3$-$MnCO_3$	?	0.50–0.52		?	≥1.14	>450	3

Note: References are 1 = Goldsmith and Heard (1961) and Reeder and Nakajima (1982); 2 = Reeder (1983); 3 = Goldsmith (1983).
* See Table 2.

Note that the 3:1 phase is always predicted to be more stable than γ-dolomite, because both are stabilized by the creation of unlike nn pairs (both between and within basal layers) and the 3:1 phase achieves a maximum number of such pairs, but γ-dolomite does not.

Solid lines in Figure 5a define regions of the parameter space ($\epsilon_{ier} = -1$, $A > 0$, $B > 0$) in which the 2:1 and 3:1 phases are predicted to be stable, and dashed lines define regions in which various metastable reactions may occur. For example, between dashed line 2:1/(C + D) and solid line 2:1/(3:1 + D), the 2:1 phase is metastable, relative to the assemblage 3:1 + D. Additional metastable boundaries are indicated by the remaining dashed lines, e.g., the line 3:1/(C_1 + C_2) defines the region in which the 3:1 phase might form from two calcite-structure phases. Double dash-dot lines separate regions in which four different phase-diagram topologies occur (Figs. 1–4). To reduce clutter, lines defining the regions in which the 5:1 phase is predicted to be stable were omitted.

Calculated phase-diagram topologies

Figures 1–4 are selected composition vs. temperature diagrams that were calculated with the TA and Equations 4a–4c. Note that a reduced temperature scale is used in which T_C is the critical temperature for disordering of stoichiometric dolomite by a second-order transition.

1. Figure 1a ($A = 3$, $B = 0$) ≡ (3,0) is a symmetric diagram with tricritical points at T_3 and T_3', but without a $C_1 + C_2$ field. Figure 1b (2.6,1) is asymmetric, but otherwise topologically equivalent to Figure 1a. If A is increased, with B held constant, the D field narrows, and T_3 and T_3' converge asymptotically.

2. Figure 2a (2.6,1.6) has tricritical points at T_3 and T_3', a eutectoid point at $T_{3\varphi}$, and a $C_1 + C_2$ field. This is referred to as the "cone" topology because of the small (unlabeled) cone-shaped D + C field at high temperature. Figure 2b compares the calculated diagram (3.2,1.7) with experimental phase-equilibrium data for the $CdCO_3$-$MgCO_3$ system (Goldsmith, 1972).

3. Figures 3a (2,1.7) and 3b (3,1.8) have tricritical points at T_3, critical end points at T_3', and $C_1 + C_2$ fields. They illustrate the "critical-end-point topology," which is the topology that is usually assumed to be correct for the $CaCO_3$-$MgCO_3$ system (e.g., Merkel and Blencoe, 1982; Carpenter, 1985).

4. Figure 4 (2.6,2) shows a diagram in which all the critical lines are metastable, and the stable C → D transition is predicted to be first order. This is referred to as the λ-metastable topology. Note that Figure 4 is topologically equivalent to the "conjectural and schematic diagram" that Goldsmith (1983) proposed for the $CaCO_3$-$ZnCO_3$ system.

It is instructive to compare Figures 1–4 with the diagrams calculated by Meijering (1963, his Figs. 1, 3, and 6), who considered a model system in which both magnetic ordering and chemical phase separation occur. There is a close, though not exact, correspondence between his results and those presented here. The essential difference is that the magnetic and chemical interaction parameters in Meijering's model can be varied independently to raise or lower the λ line relative to the miscibility gap. In the present model, however, relative positions of the λ line and the two-phase fields depend on the *ratio* $\epsilon_{ira}/\epsilon_{ier}$, so that ϵ_{ira} and ϵ_{ier} are coupled. Thus, a topology involving coexisting ordered phases (Meijering's Fig. 7) is not found in the TA, and a diagram analogous to Figure 4 does not occur in Meijering's model. Davidson and Burton (1987) have discussed a related case in which the topology with coexisting ordered phases does occur, owing to frustration in the ordered ground state.[3]

From Figures 5a and 5b, it can be seen that the cone, critical-end-point (c-e-p), and λ-metastable (λ-meta) topologies are obtained from the symmetric diagram by increasing B. It is also apparent that the transition from one topology to another is only weakly dependent on A. In Figure 5b, certain quantitative constraints are shown, and most of the 0-K lines have been removed. The dotted lines labeled 1.2, 1.1, and 1.0 are contours of constant ratio T_{cons}/T_C (where T_{cons} is the consolute temperature of the $C_1 + C_2$ field). The solid, nearly vertical curves indicate values of the parameters that are consistent with τ_C for the Ca-Mg and Cd-Mg systems [τ_C (Table 2) depends on both T_C and ΔH^{xs} ($X = 0.5$, $T \ll T_C$)]. Arrows indicate approximate locations of simultaneous fit to experimental constraints on T_C, T_{cons}, and ΔH^{xs} ($X = 0.5$, $T \ll T_C$) for the Ca-Mg and Cd-Mg systems [experimental values for T_C, ΔH^{xs}, T_{cons}/T_C were estimated from the diagrams in Goldsmith (1983), and from data in Tables 1 and 2]. Clearly, these constraints suggest that the 3:1 phase should be stable in both systems. Note, however, that with $A = 3.2$ and $B = 1.7$ (Figs. 2b and 5b), the

[3] In a system with pairwise interactions only, a frustrated ground state occurs when the geometry of the system precludes an ordered arrangement in which all nn pairs are simultaneously in their most energetically favorable configurations. For example, with equal numbers of species 1 and 2 on a two-dimensional triangular array of sites, a maximum of ⅔ of the nn's can simultaneously be in configuration 1–2.

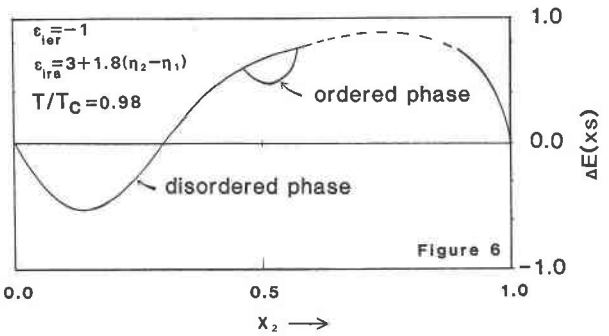

Fig. 6. Calculated curves for the excess heat of solution [$\Delta E^{xs}(X, T = 0.98T_C)$, $A = 3$, $B = 1.7$; $\Delta E^{xs} = \Delta H^{xs}$]. Note that the dolomite-structure phase (dashed curve) is stable at this temperature, even though its $\Delta E^{xs}(X,T)$ curve is everywhere greater than zero.

maximum temperature at which the 3:1 phase is predicted to be stable is about −92°C, so ordered $Cd_3Mg(CO_3)_4$ probably cannot be synthesized. The diagram in Figure 3a, which was calculated with parameters that are reasonable for the Ca-Mg system, has a C + D field that is much too narrow, and a 3:1 phase that is stable at temperatures that are much too high. This illustrates one of the quantitative limitations of the model, that low ratios of A/B (which are necessary to fit experimental constraints on T_C, T_{cons}, and ΔH^{xs}) lead to exaggerated stability for the 3:1 phase. Unfortunately, this implies that quantitative CVM-TA predictions of low-temperature $CaCO_3$-$MgCO_3$ phase relations are much less reliable than similar predictions for the $CdCO_3$-$MgCO_3$ system.

Excess heats of cation ordering

In systems that lack significant anisotropy of solution properties, $\Delta H^{xs} < 0$ (relative to mechanical mixing of endmembers) implies a tendency for ordering, and $\Delta H^{xs} > 0$ implies a tendency for phase separation. In systems characterized by strong anisotropy, however, this is not the case (Burton, 1985; Burton, 1986). In these systems, the sign of ΔH^{xs} depends very strongly on the degree of order and therefore on temperature and composition. The CVM-TA models discussed in this paper predict rather interesting systematics for the excess heats of cation ordering (Fig. 6), which can be summarized with the following inequalities:

$$\Delta H^{xs} < 0 \quad (X = 0.5,\ T < T_0) \tag{7a}$$
$$\Delta H^{xs} > 0 \quad (X = 0.5,\ T > T_0 \tag{7b}$$
$$\Delta H^{xs} < 0 \quad (X \lesssim 0.3) \tag{7c}$$

where T_0, which is generally less than T_C, is the temperature at which $\Delta H^{xs}(X,T) = 0$. Inequalities 7a and 7b are qualitatively consistent with the thermochemical measurements listed in Table 2, particularly those for $CdMg(CO_3)_2$; and 7c is qualitatively consistent with calorimetric measurements by Capobianco (1986) which revealed ΔH^{xs} ($X \leq 0.12$) < 0 in synthetic magnesian calcites.

TABLE 2. Thermochemical data pertaining to the stabilization of dolomites relative to calcite endmembers

System	T_a (°C)	S_{LRO}	$\Delta H^{xs}(X = 0.5, T)$	$\tau_C = -4kT_C/\Delta H^{xs}(0.5, 0)$
$CaMg(CO_3)_2$		1	−11.0 ± 0.4	4.15–4.30
	1200	0	3.6 ± 0.4	
$CdMg(CO_3)_2$	600	1	−5.73 ± 0.3	6.19–6.49
	750	0.66 ± 0.04	0.88 ± 0.3	
	775	0.62 ± 0.03	1.05 ± 0.3	
	850	0.05 ± 0.08	8.12 ± 0.5	

Note: T_a = the temperature at which samples were annealed before quenching. S_{LRO} = the long-range order parameter. $\Delta H^{xs}(X, T)$ is in kJ/mol. Data from Capobianco and Navrotsky (1985) and Capobianco et al. (1987).

Stability of the 3:1, γ, 2:1, δ, and 5:1 phases

Negative deviations from ideality in ΔH^{xs} of magnesian calcites imply that additional ordered phase(s) should be stable at low temperatures, but the quantitative discrepancy between experiment, ΔH^{xs} ($X \leq 0.12$) < 0, and calculation, ΔH^{xs} ($X \lesssim 0.3$) < 0, suggests that the CVM-TA exaggerates the stability of such phases. Such an exaggeration is also consistent with the discrepancy between experimental and calculated widths for the C + D field as discussed above (see Fig. 4a). Thus, thermochemical data plus the marked asymmetry of the experimental phase diagram suggests that $Ca_3Mg(CO_3)_4$ is probably stable at low temperature. Its maximum temperature of stability, as predicted by the CVM-TA however, is clearly much too high. The phase $Cd_3Mg(CO_3)_4$ is probably a stable ground state, but as discussed above, its maximum temperature of stability is probably so low as to preclude synthesis.

The γ-dolomite phase reported by Wenk and Zhang (1985) is always predicted to be less stable than the 3:1 phase, and it is plausible to regard γ as an energetically less stable, but kinetically more accessible, 3:1 phase. It should be noted, however, that TA-predicted relative stabilities of 3:1 and γ are determined by the simplistic model for many-body interactions (Eq. 4) and may therefore be artifacts of this formulation.

The 2:1 phase only occurs in a very restricted region of the parameter space, and it is unlikely to be stable. It might, however, occur as a metastable product in the low-temperature breakdown of calcian dolomite, or as a metastable precursor prior to the nucleation of dolomite from a $C_1 + C_2$ assemblage.

The δ-dolomite phase proposed by Wenk and Zhang (1985) is predicted to be more stable than the 2:1 phase, for $B \leq (3/4)(A + 1/12)$, but always metastable relative to the assemblage C + D. Because of its close structural relationship to dolomite, it is probably more kinetically accessible than the 2:1 phase, as a metastable intermediate phase in, for example, the dissolution and reprecipitation of Ca-supersaturated dolomite.

The 5:1 phase, though predicted to be stable in the same region of parameter space as the 3:1 phase, has a very low T_C (so low that attempts to calculate its stability

field failed owing to numerical underflow). Thus, the 5:1 phase is not expected to occur in nature, but short range order that is maximized at this stoichiometry is a distinct possibility.

Limitations of the CVM-TA

In the TA, Equation 4b implies a very simple form for the many-body dependence of ϵ_{ira}, one that causes the negative deviations in $\Delta H^{xs}(X)$ to be maximized at too Mg-rich a composition ($X \approx 1/6$) and causes calculated C + D fields to be much too narrow. Therefore, more complicated many-body or composition dependence is required to achieve quantitative agreement between theory and experiment; i.e., a higher-order CVM approximation or composition- and/or temperature-dependent ϵ_{ijkl} values. The essential limitation of the TA is that tetrahedra are the largest clusters, so ϵ_{ira} can only be varied in tetrahedra with compositions of $X = 1/4$, $1/2$, or $3/4$ (e.g., tetrahedra in configurations {1121}, {1122}, or {1222}, respectively). A larger cluster approximation would allow more flexibility. For example, a tetrahedron-octahedron approximation (TOA; e.g., Kikuchi, 1986) would allow one to vary ϵ_{ira} in the same tetrahedra, but also in octahedra with compositions of $X = 1/6$, $1/3$, $1/2$, $2/3$, and $5/6$. Also, it would be possible to treat ϵ_{ira} as a nonlinear function of $(\eta_2 - \eta_1)$ (Eq. 4b). With a TOA it might be possible to achieve a significantly better fit to the experimental phase-equilibrium data and to make more reliable predictions about stability fields for ordered phases other than dolomite. Alternatively, one could treat ϵ_{ier} and ϵ_{ira} as continuous nonlinear functions of composition, but this would require a different approach for solving the CVM-TA equations. In either case, however, improved agreement would be achieved, at least in part, at the expense of physical significance in the additional energy parameters that would be required.

For simplicity, the only contributions to the configurational free energy that are explicitly included in the TA are those that derive from cation ordering. Other possible contributions are ignored, e.g., rotational disordering of CO_3 groups or coupling between CO_3-group rotation and cation ordering. Ignoring these additional contributions seems justified, however, because the level of success achieved with the present formulation suggests that the most important terms have been included.

Conclusions

The principal conclusion to be drawn from the results presented above is that one can account for the high-temperature equilibrium phase relations of rhombohedral carbonates with models that incorporate two assumptions about the interactions that cause cation ordering: (1) they are highly anisotropic, such that *inter*layer interactions favor ordering, but *intra*layer interactions favor clustering; (2) there is a *strong many-body dependence* in the intralayer interactions, such that intralayer ordering is favored on one side of the phase diagram ($X \lesssim 0.3$), but intralayer clustering is favored in the remainder of the compositional range ($X \lesssim 0.3$). A three-parameter CVM-TA model, in which the energy parameters are consistent with these assumptions, is sufficient to achieve full qualitative agreement with observed high-temperature phase relations and with experimental systematics for the excess heats that are associated with cation ordering. In addition, the many-body interaction parameters that are necessary to reproduce a high-temperature $C_1 + C_2$ field also lead to the prediction that a low-temperature 3:1 phase is probably stable in the Ca-Mg system, and possibly in the Cd-Mg system as well.

Note added in proof. In the TA, the $R\bar{3}c$ 3:1 phase is degenerate with a $C2/c$ 3:1 phase having an ordered structure that is analogous to that of Al_3Ti. Basal layers of the two structures can be illustrated schematically as follows:

$R\bar{3}c$:

Ca—Mg—Ca—Mg
Ca—Ca—Ca—Ca
Ca—Mg—Ca—Mg

$C2/c$:

Ca—Mg—Ca—Mg
Ca—Ca—Ca—Ca
Mg—Ca—Mg—Ca

Adjacent layers fit together in such a way that interlayer Mg–Mg nn's are avoided. In the nonstandard $C2/a$ setting, there is a rectangular unit cell with Mg sites at its corners and C centers, and $\mathbf{a} = \mathbf{c}_h$, $\mathbf{b} = 2\mathbf{a}_h$, and $\mathbf{c} = \sqrt{3}\mathbf{a}_h$. The $R\bar{3}c$ and $C2/c$ ordering motifs can also be combined to form an infinite number of long-period superstructures (Beattie, 1967).

Acknowledgments

I wish to thank P. M. Davidson, C. Capobianco, A. Navrotsky, G. Waychunas, and E. Salje for reviews of the manuscript plus many useful discussions and suggestions. I also wish to thank C. J. Alpert, who did some of the numerical work, and the American Society for Metals, which partially supported this work.

References

Allen, S.M., and Cahn, J.W. (1982) Phase diagram features associated with multicritical points in alloy systems. Bulletin of Alloy Phase Diagrams, 3, 287–295.

Beattie, H.J., Jr (1967) Close packed structures. In J.H. Westbrook, Ed., Intermetallic compounds, 144–165. Wiley, New York.

Burton, B.P. (1985) Theoretical analysis of chemical and magnetic ordering in the system Fe_2O_3-$FeTiO_3$. American Mineralogist, 70, 1027–1035.

——— (1986) Tricritical phase relations in minerals. In L.H. Bennett, Ed. Computer modeling of phase diagrams. Metallurgical Society of AIME, 129–143.

Burton, B.P., and Kikuchi, R. (1984) Thermodynamic analysis of the system $CaCO_3$-$MgCO_3$ in the tetrahedron approximation of the cluster variation method. American Mineralogist, 69, 165–175.

Capobianco, C. (1986) Thermodynamic relations of several carbonate solid solutions. Ph.D. thesis, Arizona State University, Tempe.

Capobianco, C., and Navrotsky, A. (1985) Thermochemistry in the system $CaCO_3$-$MgCO_3$-$CdCO_3$. EOS, 66, 390.

Capobianco, C., Burton, B.P., Davidson, P.M., and Navrotsky, A. (1987) Structural and calorimetric studies of order-disorder in $CdMg(CO_3)_2$, in press. Journal of Solid State Chemistry.

Carpenter, M.A. (1985) Order-disorder transformations in mineral solid

solutions. Mineralogical Society of America Reviews in Mineralogy, 14, 187–218.

Davidson, P.M., and Burton, B.P. (1987) Order-disorder in omphacitic pyroxenes: A model for coupled substitution in the point approximation. American Mineralogist, 72, 337–344.

Goldsmith, J.R. (1972) Cadmium dolomite and the system $CdCO_3$-$MgCO_3$. Journal of Geology, 80, 611–626.

——— (1983) Phase relations of rhombohedral carbonates. Mineralogical Society of America Reviews in Mineralogy, 11, 49–76.

Goldsmith, J.R., and Heard, H.C. (1961) Subsolidus phase relations in the system $CaCO_3$-$MgCO_3$. Journal of Geology, 69, 453–457.

Kikuchi, R. (1986) The CVM calculation of phase diagrams. In L.H. Bennett, Ed. Computer modeling of phase diagrams. Metallurgical Society of AIME, 49–65.

Meijering, J.L. (1963) Miscibility gaps in ferromagnetic alloy systems. Philips Research Reports, 18, 318–330.

Merkel, G.A., and Blencoe, J.G. (1982) Thermodynamic procedures for treating the monoclinic/triclinic inversion as a high-order phase transition in equations of state for binary analbite-sanidine feldspars. In S.K. Saxena, Ed. Advances in physical geochemistry, vol. 2. Springer-Verlag, New York.

Reeder, R.J. (1983) Crystal chemistry of the rhombohedral carbonates. Mineralogical Society of America Reviews in Mineralogy, 11, 49–76.

Reeder, R.J., and Nakajima, Y. (1982) The nature of ordering and ordering defects in dolomite. Physics and Chemistry of Minerals, 8, 29–35.

Van Tendeloo, G., Wenk, H.R., and Gronsky, R. (1985) Modulated structures in calcian dolomite: A study of electron microscopy. Physics and Chemistry of Minerals, 12, 333–341.

Wenk, H.R., and Zhang, F. (1985) Coherent transformations in calcian dolomites.Geology, 13, 457–460.

Manuscript received July 14, 1986
Manuscript accepted December 2, 1986